https://doi.org/10.3311/PPch.21743

Periodica Polytechnica Chemical Engineering, 67(3), pp. 407–415, 2023

Kinetics, Equilibrium and Thermodynamic Studies on Removal of Oleic Acid from Sunflower Oil onto Amberlyst A21

Oguzhan Ilgen[1*], Elif Tümkor[1]

[1] Chemical Engineering Department, Engineering Faculty, Kocaeli University, Umuttepe Campus, 41380 Izmit, Kocaeli, Türkiye
[*] Corresponding author, e-mail: oilgen@kocaeli.edu.tr

Received: 23 December 2022, Accepted: 02 March 2023, Published online: 19 July 2023

Abstract

Amberlyst A21 was used for the oleic acid adsorption from sunflower oil (SFO). The impacts of parameters such as contact time, temperature, and mass ratio of adsorbent on oleic acid adsorption were studied. The characterization of Amberlyst A21 before and after adsorption was performed by using Fourier transform infrared spectrometer (FTIR) and scanning electron microscope (SEM). The adsorption reached equilibrium 480 minutes later. The increase in temperature and the amount of adsorbent caused an increase in the amount of adsorbed oleic acid. The adsorption kinetics, isotherms, and thermodynamics were studied. The pseudo-first order kinetics well described the adsorption for all studied temperatures. The Langmuir, Freundlich, and Dubinin−Radushkevich isotherms and thermodynamic analysis were investigated at equilibrium. The suitability of the Langmuir and Freundlich isotherms indicated that the adsorption takes place under monolayer and heterogeneous surfaces. Thermodynamical results showed that adsorption occurs spontaneously and endothermic.

Keywords

Amberlyst A21, adsorption, oleic acid, kinetics, equilibrium

1 Introduction

A large amount of waste cooking oil is produced as a by-product from frying in homes, restaurants, and catering companies. Most of the waste vegetable oils (WVOs) cause environmental pollution and economic problems. The WVOs that mix with the sewer as a result of pouring into the sink cause a vast amount of damage to the sewer systems around the world. The WVOs also cause a significant threat to public health [1]. Biodiesel production from WVOs is an environmentally friendly and economically effective method for WVOs assessment [2]. WVOs are relatively low cost and rich in free fatty acid (FFA) content. Biodiesel can be produced by mixing the oil with alcohol using a catalyst. The main disadvantage of producing biodiesel with a basic catalyst is that the FFA content in the oil causes soap formation and reduces the reaction efficiency. It also prevents the separation of biodiesel from glycerine after the reaction. In the case of using an acid catalyst in biodiesel production, the disadvantages are slower reaction and corrosion in the equipment involved [2–4].

It is possible that the use of WVOs in biodiesel production can be efficient and viable by reducing the FFA content. There are some possible common processes such as distillation, extraction, and esterification to reduce the FFA content of WVOs. Adsorption is a preferred alternative because distillation takes place at high temperatures and a significant amount of solvent is required for extraction [5, 6].

The studies carried out so far include the use of various adsorbents to capture FFA from WVOs. In literature, the use of different types of resins has been investigated within the scope of studies about the adsorption of FFAs. Jamal and Boulanger [7] investigated the removal of oleic acid from soybean oil on Dowex MR-450 UPW and Amberlyst MB-150 resins. Maddikeri et al. [8] studied the removal of stearic acid and oleic acid from SFO on Indion 810, 850, and 860. In the study performed by Ilgen [9], Amberlyst A26 (OH) was researched for the oleic acid adsorption from SFO. It was also used in another study by Deboni et al. [10] for the linoleic acid adsorption from a mixture of soybean oil and ethanol. In addition, Singh et al. [5] researched the adsorption of palmitic, stearic and oleic acid from soybean oil separately onto different type Amberlite resins as adsorbent. Khedkar et al. [11]

Cite this article as: Ilgen, O., Tümkor, E. "Kinetics, Equilibrium and Thermodynamic Studies on Removal of Oleic Acid from Sunflower Oil onto Amberlyst A21", Periodica Polytechnica Chemical Engineering, 67(3), pp. 407–415, 2023. https://doi.org/10.3311/PPch.21743

researched the effect of silver load on resins for removal of oleic acid from various solvents on HP20, Indion 860, Indion 790. Other than, different types of materials were also used as adsorbents. Cano et al. [12] used iron oxide nanoparticles for the adsorption of oleic acid from SFO and olive oil. Narachai et al. [13] researched the adsorption of oleic acid from isooctane onto MCM-41 synthesized from rice husk silica. Miyashiro et al. [14] investigated the removal of FFAs in edible oil on bentonite and sugarcane bagasse. It has been observed that the effects of various experimental parameters, kinetics, isotherms, and thermodynamics were investigated in the previously cited studies and similar studies not included here. The results obtained are discussed in the next parts of this study.

Although the utilization of Amberlyst A21 as an adsorbent for removal of various substances from different solutions has been investigated in the literature [15–20], no study has been found for the adsorption of oleic acid from vegetable oils. In this work, adsorption of oleic acid was performed by using Amberlyst A21 from oleic acid-SFO solution. The impacts of time, temperature, and mass ratio of adsorbent on oleic acid adsorption were investigated. Pseudo-first and pseudo-second order kinetics, Langmuir, Freundlich, and Dubinin-Radushkevich (D-R) isotherms and thermodynamics of adsorption were studied.

2 Experimental

2.1 Materials

SFO was purchased from a local market. Waste SFO was provided from local restaurant. Oleic acid, potassium hydroxide, diethyl ether and ethanol were purchased from Merck. Amberlyst A21 was purchased from Sigma-Aldrich. The properties of Amberlyst A21 was presented in Table 1.

2.2 Characterization methods of adsorbent

FTIR analysis of Amberlyst A21 were performed before and after adsorption by using PerkinElmer ATR - FTIR spectrophotometer 650–4000 cm^{-1} at room temperature. The SEM images of Amberlyst A21 before and after adsorption were obtained by using Zeiss EVO-5 SEM.

Table 1 Typical properties of Amberlyst A21 [21]

Form	Beads
Moisture	56–62%
Matrix	styrene-divinylbenzene (macroporous)
Matrix active group	dimethylamino
Particle size	22–30 mesh, 490–690 μm
Capacity	1.3 meq/mL by wetted bed volume

2.3 Experiments and analysis

The solution was prepared by adding the required amount of oleic acid to SFO to provide 3% oleic acid by weight in the solution. 50 grams of solution in a beaker was used in each experiment. Experiments were carried out at temperatures of 303 K, 323 K, and 343 K. After the solution reached the desired temperature, the adsorbent was added to the solution. The adsorbent amounts of 15%, 20%, and 25% were used based on the solution weight. The experiments were carried out at a stirring speed of 500 rpm.

Samples were taken at certain time intervals and centrifuged. The sample was added in a 50/50 volume percent ethanol-diethyl ether solution to better dissolve the oleic acid and SFO. Afterwards, a few drops of phenolphthalein were added and titration was performed with 0.01 N KOH solution. Experiments were repeated three times for each data and mean values were used. The titration and calculations were performed in accordance with The American Oil Chemists' Society Method Cd 30-63. The oleic acid concentration, adsorbed amount, and percentage of oleic acid in the sample were calculated with the help of Eqs. (1)–(3):

$$C = \frac{V_{KOH} C_{KOH} MW_{OA}}{m_N}, \tag{1}$$

where C is oleic acid concentration in the mixture (mg/g), V_{KOH} is the volume of KOH used in titration (ml), C_{KOH} is KOH concentration (mol/l), m_N is sample weight (g) and MW_{OA} is oleic acid molecular weight (g/mol).

$$q = \frac{(C_0 - C_t) M}{W}, \tag{2}$$

$$\text{Oleic acid removal } (\%) = \frac{(C_0 - C_t)}{C_0} \times 100, \tag{3}$$

where q is the amount of oleic acid adsorbed per gram of adsorbent (mg/g), C_0 is the initial concentration of oleic acid (mg/g), C_t is the concentration of oleic acid at time t (mg/g), M is the mass of the mixture (g), and W is the mass of adsorbent (g).

The desorption percentage amount was determined using Eq. (4):

$$\text{Desorption } (\%) = \frac{q_D}{q} \times 100, \tag{4}$$

where q_D is the amount of oleic acid desorbed per adsorbent amount (mg oleic acid/g adsorbent).

3 Results and discussion

3.1 Adsorbent characterization

FTIR spectra of Amberlyst A21 before and after adsorption are shown in Fig. 1. The characteristic peaks of Amberlyst 21 are seen at 2930, 2810, and 2770 cm^{-1} as the C-H stretching vibration of alkane and aldehyde. The C-N stretching vibration of the amine is observed at 1362 cm^{-1}. There are also bands characterizing the bending vibrations of the alkene in the ranges of 1600–1400 and 1000–675 cm^{-1}. The characteristic peaks of the Amberlyst 21 and the peaks of oleic acid appeared in close proximity, the peaks appeared as larger peaks of oleic acid after adsorption. In the spectra of the resin after adsorption, peaks belonging to oleic acid were observed at 2923 cm^{-1} and 2853 cm^{-1}, which were considered to belong to asymmetric CH_2 stretching and symmetrical CH_2 stretching, respectively. The peak at 1744 cm^{-1} corresponds to the C=O stretch. In the literature, after the adsorption of oleic acid to different adsorbents, the same oleic acid peaks in close proximity to each other were observed in all studies, regardless of the adsorbent type. The literature states that it can be used to determine the initial concentration of oleic acid from the area of C–H stretch bands in the range of 2800–3000 cm^{-1} in the FTIR analysis [12, 19]. These evaluations show us that oleic acid is adsorbed on the Amberlyst A21 surface. SEM was used to investigate the morphology of Amberlyst A21. The SEM images of Amberlyst A21 surfaces are presented in Fig. 2 (a) and (b) before and after adsorption, respectively. Before oleic acid adsorption, Amberlyst A21 had a smooth surface as seen in Fig. 2 (a), while oleic acids appeared on the surface of Amberlyst A21 beads after adsorption as seen in Fig. 2 (b).

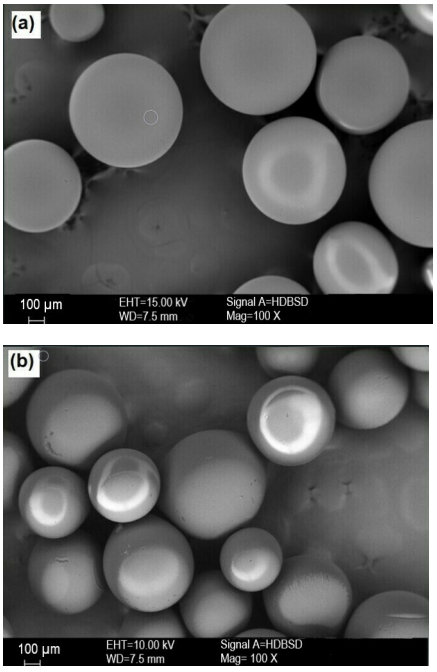

Fig. 2 SEM images of Amberlyst A21 (a) before adsorption; (b) after adsorption

3.2 Impact of parameters

The impact of contact time and temperature for oleic acid removal from SFO on Amberlyst A21 was studied. As depicted in Fig. 3, gradually increased adsorption of oleic acid was observed at temperatures of 303 K, 323 K, and 343 K and at a constant adsorbent amount of 15%. The adsorption reached equilibrium 480 minutes later for all studied temperatures.

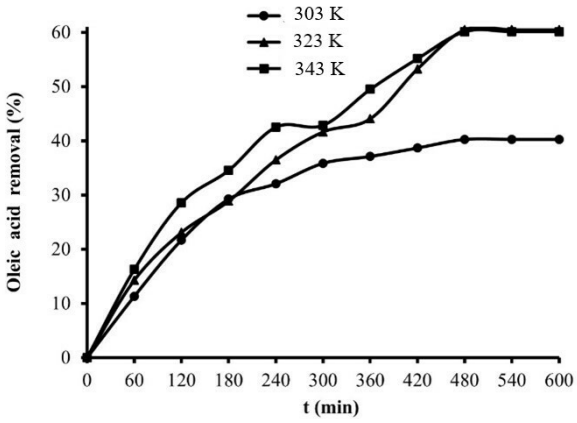

Fig. 3 Impact of contact time and temperature

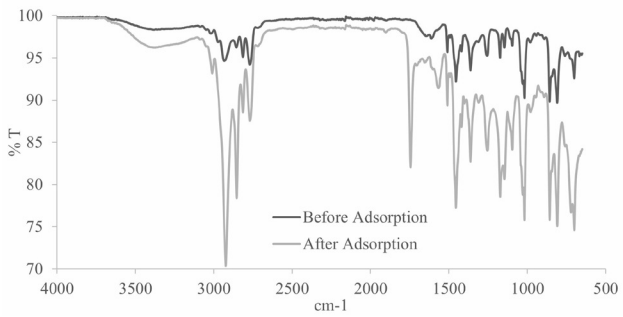

Fig. 1 FTIR spectra of Amberlyst A21 before and after adsorption

The impact of the amount of adsorbent at the different temperatures at equilibrium is presented in Fig. 4. Experiments were performed at temperatures of 303 K, 323 K and 343 K using 15%, 20%, and 25% adsorbent amounts for each temperature. The increase in temperature and the amount of adsorbent increased the removal of oleic acid (see Fig. 4). The maximum oleic acid removal was observed as 75.4% at temperature of 323 K and using 25% adsorbent amount. The increase in adsorption with temperature indicates that the process is endothermic.

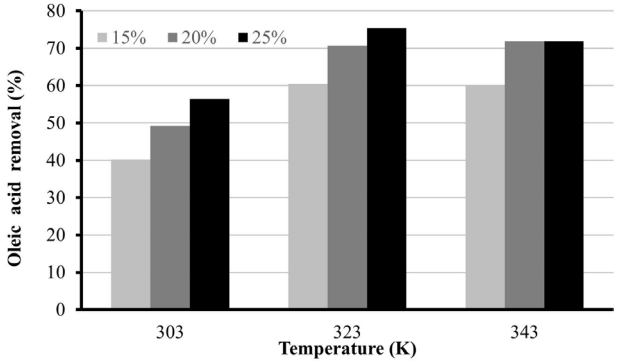

Fig. 4 Impact of temperature and adsorbent amount

3.3 Adsorption kinetics

The adsorption kinetics of the oleic acid–SFO solution was investigated by using pseudo-first and pseudo-second-order kinetic models.

Lagergren presented a pseudo-first-order rate equation based on adsorption capacity to describe the kinetic process of liquid-solid phase adsorption. The linear form of Eq. (5) is as follows [22]:

$$\log\left(q_e - q_t\right) = \log q_e - \frac{k_1}{2.303}t, \tag{5}$$

where q_e is the adsorption capacities at equilibrium (mg/g), q_t is the adsorption capacities at time t (mg/g), k_1 is the first order rate constant (min^{-1}).

When plotting $\log(q_e - q_t)$ versus t, the slope of the graph gives the k value and the intercept gives the calculated $q_{e\text{-cal}}$ value.

The linearized pseudo-second order model presented as [23]:

$$\frac{t}{q_t} = \frac{1}{k_2 q_e^2} + \frac{t}{q_e}, \tag{6}$$

where k_2 is the second order rate constant (g/mg min).

When plotting (t/q_t) versus t, $q_{e\text{-cal}}$ and k_2 values can be determined from slope and intercept of lines.

The data obtained for temperatures of 303 K, 323 K, 343 K and adsorbent amounts of 15%, 20%, 25% were calculated by using Eqs. (5) and (6) and transferred to the graph. The k_1, k_2, theoretical q_e values and kinetic equations determined from the graphs are given in Table 2. R^2 values, theoretical q_e, and experimental q_e values were determined and the compatibility of the kinetic models were evaluated. As depicted in Table 2, when R^2 values

Table 2 Kinetic parameters and equations of oleic acid adsorption on to Amberlyst A21

Ads.% (w/w)	$q_{e\text{-exp}}$ (mg/g)	Pseudo-first order			Pseudo-second order		
		k_1 (min^{-1})	$q_{e\text{-cal}}$ (mg/g)	R^2	k_2 (g/mg min)	$q_{e\text{-cal}}$ (mg/g)	R^2
			T = 303 K				
15	85.33	0.0074	90.95	0.99	0.000040	121.95	0.98
			$y = -0.0032x + 1.9588$			$y = 0.0082x + 1.6619$	
20	80.00	0.0067	79.09	0.98	0.000063	104.17	0.98
			$y = -0.0029x + 1.8981$			$y = 0.0096x + 1.471$	
25	70.00	0.0032	69.04	0.93	0.000012	136.99	0.70
			$y = -0.0014x + 1.8391$			$y = 0.0073x + 4.2842$	
			T = 323 K				
15	132.67	0.0044	141.94	0.94	0.0000082	250.00	0.91
			$y = -0.0019x + 2.1521$			$y = 0.004x + 1.9536$	
20	106.00	0.0062	151.00	0.70	0.0000025	344.83	0.65
			$y = -0.0027x + 2.1790$			$y = 0.0029x + 3.3451$	
25	92.00	0.0051	114.57	0.70	0.0000086	188.68	0.54
			$y = -0.0022x + 2.0591$			$y = 0.0053x + 3.2373$	
			T = 343 K				
15	120.67	0.0053	126.65	0.95	0.000018	188.68	0.97
			$y = -0.0023x + 2.1026$			$y = 0.0059x + 1.488$	
20	108.50	0.0062	129.54	0.95	0.000013	196.08	0.98
			$y = -0.0027x + 2.1124$			$y = 0.0051x + 2.0467$	
25	92.00	0.0067	117.06	0.91	0.000013	175.44	0.97
			$y = -0.0029x + 2.0684$			$y = 0.0057x + 2.5942$	

were evaluated, pseudo-first order kinetic was found suitable for temperatures of 303 K and 323 K. For the pseudo-first order model, along with the higher R^2 values at 303 K and 323 K the theoretical q_e values were also found to be more consistent with the experimental data. Although the R^2 values for the pseudo-second and pseudo-first order can be considered close to each other at 343 K, it was seen that the theoretical q_e and the experimental q_e values for pseudo-first order models were in better agreement. As a result, it was evaluated that the pseudo-first order model was more suitable for all studied temperatures.

In the literature, oleic acid adsorption onto Zeolite 13X was investigated by Ilgen and Dulger [24], it was found that it was suitable for pseudo-second order kinetics at 323 K and 343 K, and suitable for both pseudo-first and pseudo-second order kinetics at 303 K. In another study by Maddikeri et al. [8], it was reported that the removal of oleic and stearic acid from SFO onto resins was compatible with pseudo-first order kinetics. Cano et al. [12] studied the removal of oleic acid from SFO and olive oil on iron oxide nanoparticles. It was observed that the adsorption conformed to the pseudo-second order kinetics. Jamal et al. [25] found that it complied with the pseudo-first order kinetic in their study of adsorption of oleic acid on Dowex MR-450 using soybean oil. Deboni et al. [10] studied the adsorption of FFAs from soybean oil on Amberlyst A26 OH. It was found to fit the pseudo-first and pseudo-second order kinetics.

3.4 Adsorption isotherms

Different isotherm models were used to explain the adsorption process which describe the interrelation with adsorbent and adsorbate in equilibrium. The isotherms of oleic acid on Amberlyst A21 were obtained using equilibrium values at each studied temperature (303 K, 323 K, 343 K) and with each studied adsorbent ratio (15%, 20%, 25%). The conformity of Langmuir, Freundlich, and D-R isotherms with the experimental data was evaluated. The graphs obtained for Langmuir isotherm, Freundlich isotherm and D-R isotherms are presented in Figs. 5–7, respectively. The calculated constants from the different isotherms are presented in Table 3.

The linear form of Langmuir isotherm can be expressed as [26]:

$$\frac{1}{q_e} = \frac{1}{q_m} + \frac{1}{bq_m C_e}, \tag{7}$$

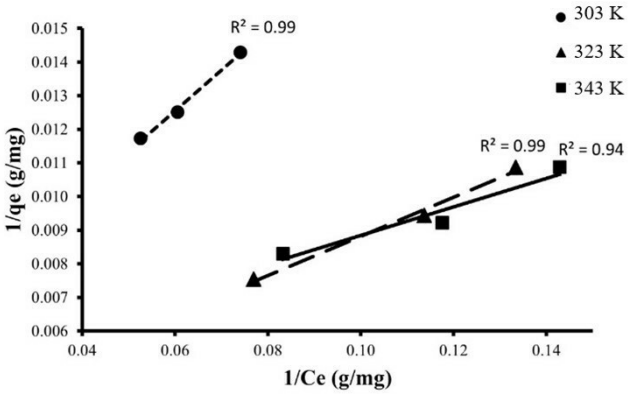

Fig. 5 Langmuir isotherms of adsorption of oleic acid on Amberlyst A21

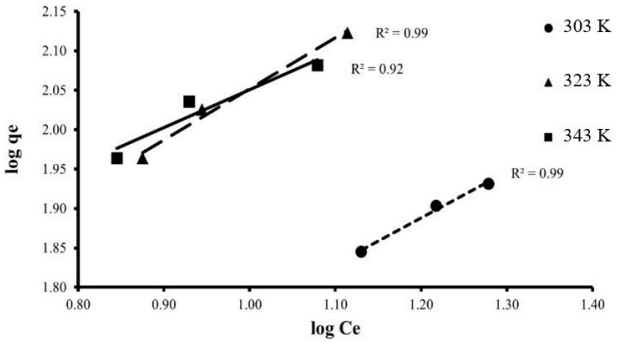

Fig. 6 Freundlich isotherms of adsorption of oleic acid on Amberlyst A21

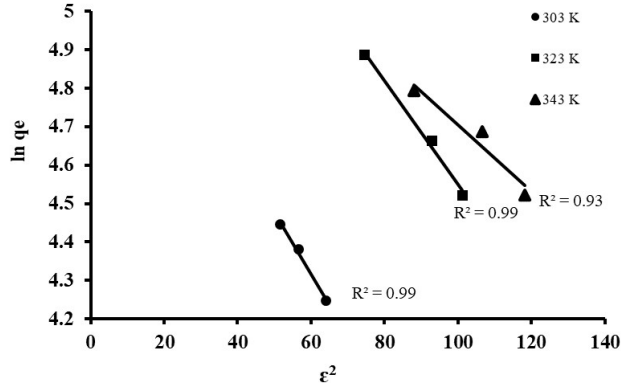

Fig. 7 D-R isotherms of adsorption of oleic acid on Amberlyst A21

Table 3 Isotherm parameters for adsorption of oleic acid on Amberlyst A21

T (K)	Langmuir		Freundlich		D-R		
	q_m (mg/g)	b (g/mg)	k_F	n	B	q_s (mg/g)	E (kJ/mol)
303	188.68	0.044	15.33	1.71	0.016	196.74	5.57
323	333.33	0.052	25.30	1.54	0.013	362.17	6.11
343	217.39	0.108	37.14	2.08	0.009	262.15	7.62

where q_m is the maximum adsorption capacity (mg/g), C_e is the concentration of substance remaining in solution (mg/g), b is the Langmuir constant (g/mg).

The K_L values were calculated using the b value obtained from the Langmuir isotherm ($K_L = (1 + bC_0)^{-1}$; C_0: concentration at $t = 0$). The calculated K_L values (0.41; 0.38; 0.23) are in the range of 0–1 for temperature of 303 K, 323 K and 343 K, respectively. The K_L values which are between 0 and 1 indicates that the adsorption is compatible with the Langmuir isotherm.

The linear form of Freundlich isotherm is represented as [27]:

$$\log q_e = \log k_F + \frac{1}{n}\log C_e, \tag{8}$$

where n and k_F values are constants isotherm constants. They were obtained as 1.7, 1.54 and 2.08 for temperature of 303 K, 323 K, 343 K, respectively. The fact that $n > 1$ means that the adsorption is physical. The k_F values which are the measure of the adsorption capacity were calculated as 15.33, 25.30, and 37.14 for temperatures of 303 K, 323 K, 343 K, respectively. It can be stated that the k_F values increase with the increase in temperature, thus the adsorption capacity also increases with the temperature.

The linear form of D-R isotherm can be expressed as [28]:

$$\ln q_e = \ln(q_s) - (B\varepsilon^2), \tag{9}$$

where q_s is the theoretical isotherm saturation capacity (mg/g), B is the isotherm constant (mol²/kJ²), ε is the Polanyi potential (kJ/mol).

The ε is calculated using Eq. (10):

$$\varepsilon = RT\ln\left[1 + \frac{C^0}{C_{e(D-R)}}\right], \tag{10}$$

where R is the universal gas constant (8.314 J/mol K), T is the absolute temperature, C^0 is the concentration of the solution in the chosen standard state (1 mol/L), $C_{e(D\text{-}R)}$ is the equilibrium concentration of solution (mol/L). In the context of the D-R isotherm analysis, it is important to acknowledge that the concentration units employed for C_e were expressed in mol/L, as proposed by Zhou [29] in 2020.

The constants of B and q_s values were determined from the slope and intercept in Fig. 7 which plotted according to Eq. (9). E is mean free energy values, which give information about whether the adsorption process is physical or not, were calculated by using Eq. (11):

$$E = (2B)^{-0.5}. \tag{11}$$

If the E values are between 8–19 kJ/mol, it is considered that the adsorption is chemical. Otherwise, if it is less than 8 kJ/mol, it is considered to be physical adsorption [24]. In current work, the E values were determined as 5.57, 6.11, 7.62 kJ/mol for temperatures of 303 K, 323 K and 343 K, respectively. Since the calculated E values are less than 8 kJ/mol, it can be stated that the adsorption of oleic acid on Amberlyst A21 is physical adsorption.

When the Langmuir, Freundlich and D-R isotherm models were evaluated together, it was seen that the R^2 values were higher than 0.9 for all models, and all models were considered suitable for describing adsorption. According to the Langmuir and Freundlich isotherms, adsorption takes place under monolayer and heterogeneous surfaces [30]. The D-R isotherm is used to describe whether adsorption is physical or chemical. Consistent with each other, the fact that the Freundlich isotherm constants n is greater than 1 and the E values determined from D-R isotherms is less than 8 kJ/mol showed that the adsorption is physical [31]. An increase in both the q_m value for the Langmuir isotherm and the q_s value for the D-R isotherm is observed as the temperature rises from 303 K to 323 K. It is seen that the qm and qs values for the Langmuir and D-R isotherms decrease at 343 K. The reduction in q_m for the Langmuir isotherm can be attributed to the reduction in the maximum capacity for monolayer adsorption of oleic acid compared to the temperature of 323 K. Similarly, in the case of the D-R isotherm, it is observed that as the temperature reaches 343 K, the q_s value decreases, signifying a reduction in the saturation capacity of the adsorbent when compared to the temperature of 323 K. In contrast to the Langmuir and D-R isotherms, it is notable that the Freundlich adsorption capacity constant, k_F, exhibits an increase with rising in all studied temperature. This increase implies that adsorption takes place on heterogeneous surfaces, leading to an augmented adsorption capacity as the temperature escalates. Furthermore, the elevation of adsorption with temperature suggests an endothermic nature of the process.

The oleic acid adsorption from soybean oil onto ion exchange resins was investigated by Jamal et al. [25]. High R^2 values were obtained for Langmuir ($R^2 = 0.99$) and Freundlich ($R^2 = 1$) isotherms. Maddikeri et al. [8] investigated the removal of oleic and stearic acid from SFO on ion exchange resins and obtained high R^2 values for Langmuir ($R^2 = 0.93$) and Freundlich ($R^2 = 1$) isotherms. The R^2 values of Langmuir ($R^2 = 0.94$) and Freundlich ($R^2 = 1$) isotherms were obtained by Ilgen [9] for the removal of oleic acid from SFO on Amberlyst A26 and it was stated that the data fit the Freundlich isotherm better.

3.5 Thermodynamic analysis

The enthalpy, entropy, and free energy changes that occur during the adsorption were investigated. The thermodynamic distribution coefficient K, which is expressed mathematically by the following equation in adsorption processes [8]:

$$\lim_{C\to 0}\left(q_e/C_e\right)=K\,. \tag{12}$$

To calculate the thermodynamic distribution coefficient K, C_e versus $\ln(q_e/C_e)$ was plotted separately for each studied temperature, and K values were calculated from the intercept [32]. The plot for the determination of K values were presented in Fig. 8. The points are used to determine a straight line, and its intersection with the vertical axis provides the K value, which is also supported by previous studies [8, 32]. The Gibbs Free Energy was calculated by using the determined K values in Eq. (13).

$$\Delta G^\circ=-RT\ln K \tag{13}$$

$$\ln K=\frac{\Delta S^\circ}{R}-\frac{\Delta H^\circ}{RT} \tag{14}$$

The entropy and enthalpy values of the adsorption were determined by using the Van't Hoff equation (Eq. (14)). A straight line was obtained by plotting $1/T$ (K^{-1}) versus $\ln K$. The ΔH° value was calculated from the slope of this line ($-\Delta H^\circ/R$), and the entropy value ΔS° from the intercept ($\Delta S^\circ/R$) (Fig. 9). The calculated K, ΔH° (kJ/kmol), ΔG° (kJ/mol), and ΔS° (kJ/mol K) values for the adsorption are given in Table 4.

Considering the data in Table 4, it is seen that negative ΔG° values indicate that adsorption occurs spontaneously under experimental conditions. The positive ΔS° value again indicates that the adsorption takes place spontaneously while the positive ΔH° indicates

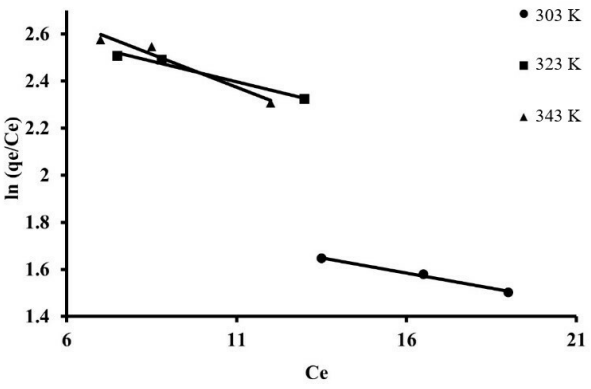

Fig. 8 Plots of $\ln(q_e/C_e)$ vs. C_e for the oleic acid adsorption on the Amberlyst A21

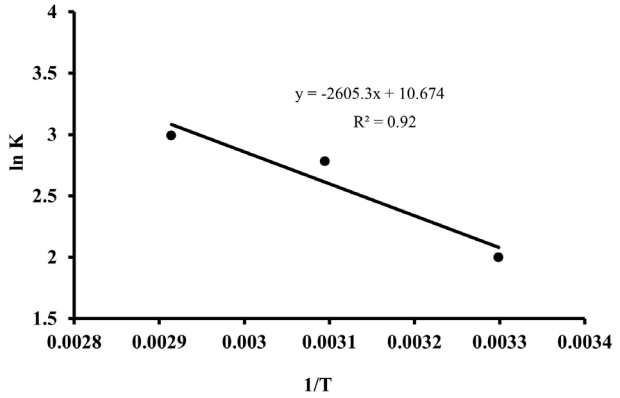

Fig. 9 Van't Hoff plot for the oleic acid adsorption on the Amberlyst A21

Table 4 Thermodynamic parameters for adsorption of oleic acid on to Amberlyst A21

T (K)	K	ΔG° (kJ/mol)	ΔS° (kJ/mol K)	ΔH° (kJ/mol)
303.15	7.39	−5.04		
323.15	16.13	−7.47	0.088	21.66
343.15	19.91	−8.53		

that the adsorption is endothermic. The positive value of ΔH° is also consistent with the results examining the effect of temperature. Maddikeri et al. [8] reported that the adsorption was exothermic where they performed the adsorption of oleic and stearic acid from SFO onto resins. Jamal et al. [25] observed that the removal of oleic acid on Dowex MR-450 using soybean oil was endothermic. Ilgen and Dulger [24] determined that removal of oleic acid from SFO using Zeolite 13X was endothermic.

3.6 Desorption studies

Adsorption of oleic acid from a 20% adsorbent ratio of oleic acid-SFO mixture on Amberlyst A21 was carried out at 303 K in order to use in the desorption study. After the resin was filtered, the adsorbed oleic acid was desorbed from Amberlyst A21 using 75 ml ether – 75 ml ethanol solution at 303 K. It was observed that 77.2% of the adsorbed oleic acid was desorbed by using 75 ml ether – 75 ml ethanol solution.

3.7 Adsorption studies using waste oil

FFA content of waste SFO was determined as 0.8% which supplied from a local restaurant. Adsorption experiments were performed at 303 K, 323 K and 343 K temperatures and using 20% adsorbent amount for 480 minutes, and the results were compared with the model waste oil under the same conditions. The obtained results are depicted in Fig. 10. Adsorption was observed to be less in waste

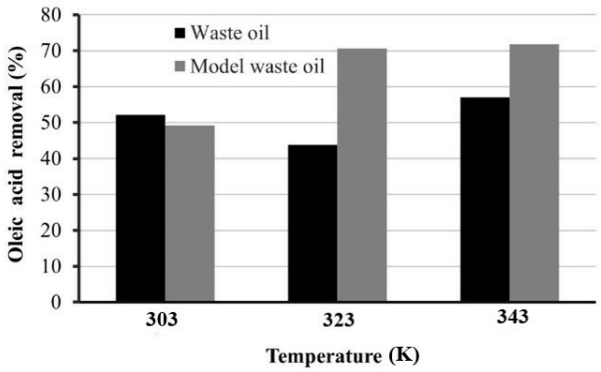

Fig. 10 Oleic acid removal from restaurant waste oil and model waste oil

restaurant oil than in model waste oil. It was thought that the impurities in the waste oil taken from the local restaurant caused this situation.

4 Conclusions

The adsorption of oleic acid added to SFO was carried out by using Amberlyst A21 as an adsorbent. The adsorption reached equilibrium 480 minutes later for all studied temperatures and it was observed that the amount of oleic acid increased as a result of increasing the amount of adsorbent and temperature. The highest oleic acid removal was observed as 75.4%. As a result of the examination of the adsorption kinetics, it was considered that the pseudo-first-order kinetics was more appropriate for all temperatures studied. According to the Langmuir and Freundlich isotherms, adsorption takes place under monolayer and heterogeneous surfaces. The calculated E values from D-R isotherms are less than 8 kJ/mol, it can be stated that the removal of oleic acid onto Amberlyst A21 is physical adsorption. Thermodynamical results showed that adsorption occurs spontaneously because negative $\Delta G°$ and positive $\Delta S°$ values obtained, and it is an endothermic process since positive $\Delta H°$ value. The 77.2% of the adsorbed oleic acid was desorbed by using 75 ml ether – 75 ml ethanol solution. It was observed that in the case of using local restaurant oil, less adsorption took place compared to the model waste oil.

References

[1] Sangkharak, K., Klomklao, S., Paichid, N., Yunu, T. "Statistical optimization for fatty acid reduction in waste cooking oil using a biological method and the continuous process for polyhydroxyalkanoate and biodiesel production", Biomass Conversion and Biorefinery, 2021. https://doi.org/10.1007/s13399-021-01756-8

[2] Topare, N. S., Patil, K. D. "Biodiesel from waste cooking soybean oil under ultrasonication as an alternative fuel for diesel engine", Materials Today: Proceedings, 43, pp. 510–513, 2021. https://doi.org/10.1016/j.matpr.2020.12.025

[3] Elgharbawy, A. S., Sadik, W. A., Sadek, O. M., Kasaby, M. A. "Maximizing biodiesel production from high free fatty acids feedstocks through glycerolysis treatment", Biomass and Bioenergy, 146, 105997, 2021. https://doi.org/10.1016/j.biombioe.2021.105997

[4] Ekin, İ. "Quality and composition of lipids used in biodiesel production and methods of transesterification: A review", International Journal of Chemistry and Technology, 3(2), pp. 77–91, 2019. https://doi.org/10.32571/ijct.623165

[5] Singh, R., Dien, B. S., Singh, V. "Response surface methodology guided adsorption and recovery of free fatty acids from oil using resin", Biofuels, Bioproducts & Biorefining, 15(5), pp. 1485–1495, 2021. https://doi.org/10.1002/bbb.2255

[6] Díaz, L., Mertes, L., Brito, A., Rodríguez, K. E. "Valorization of energy crop shells as potential green adsorbents for free fatty acid removal from oils for biodiesel production", Biomass Conversion and Biorefinery, 12(3), pp. 655–668, 2022. https://doi.org/10.1007/s13399-020-01089-y

[7] Jamal, Y., Boulanger, B. O. "Separation of Oleic Acid from Soybean Oil Using Mixed-bed Resins", Journal of Chemical & Engineering Data, 55(7), pp. 2405–2409, 2010. https://doi.org/10.1021/je900829c

[8] Maddikeri, G. L., Pandit, A. B., Gogate, P. R. "Adsorptive Removal of Saturated and Unsaturated Fatty Acids Using Ion-Exchange Resins", Industrial & Engineering Chemistry Research, 51(19), pp. 6869–6876, 2012. https://doi.org/10.1021/ie3000562

[9] Ilgen, O. "Adsorption of Oleic Acid from Sunflower Oil on Amberlyst A26 (OH)", Fuel Processing Technology, 118, pp. 69–74, 2014. https://doi.org/10.1016/j.fuproc.2013.08.012

[10] Deboni, T. M., Hirata, G. A. M., Shimamoto, G. G., Tubino, M., de Almeida Meirelles, A. J. "Deacidification and ethyl biodiesel production from acid soybean oil using a strong anion exchange resin", Chemical Engineering Journal, 333, pp. 686–696, 2018. https://doi.org/10.1016/j.cej.2017.09.107

[11] Khedkar, M. A., Satpute, S. R., Bankar, S. B., Chavan, P. V. "Adsorptive removal of unsaturated fatty acids using ion exchange resins", Journal of Chemical & Engineering Data, 66(1), pp. 308–321, 2020. https://doi.org/10.1021/acs.jced.0c00700

[12] Cano, M., Sbargoud, K., Allard, E., Larpent, C. "Magnetic Separation of Fatty Acids with Iron Oxide Nanoparticles and Application to Extractive Deacidification of Vegetable Oils", Green Chemistry, 14(6), pp. 1786–1795, 2012. https://doi.org/10.1039/C2GC35270B

[13] Narachai, B., Kajsanthia, K., Osakoo, N., Wittayakun, J., Prayoonpokarach, S. "Adsorption of Oleic Acid Using MCM-41 Synthesized from Rice Husk Silica", [pdf] Suranaree Journal of Science & Technology, 25(1), pp. 37–48, 2018. Available at: https://www.thaiscience.info/Journals/Article/SJST/10989673.pdf [Accessed: 22 December 2022]

[14] Miyashiro, C. S., Bonassa, G., Schneider, L. T., Parisotto, E. I. B., Alves, H. J., Teleken, J. G. "Evaluation of different adsorbents for acidity reduction in residual oils", Environmental Technology, 40(11), pp. 1438–1454, 2019. https://doi.org/10.1080/09593330.2017.1422807

[15] Hubicki, Z., Wołowicz, A. "Adsorption of palladium(II) from chloride solutions on Amberlyst A 29 and Amberlyst A 21 resins", Hydrometallurgy, 96(1–2), pp. 159–165, 2009. https://doi.org/10.1016/j.hydromet.2008.10.002

[16] Guimarães, D., Leão, V. A. "Batch and fixed-bed assessment of sulphate removal by the weak base ion exchange resin Amberlyst A21", Journal of Hazardous Materials, 280, pp. 209–215, 2014. https://doi.org/10.1016/j.jhazmat.2014.07.071

[17] Sarı, S. K., Özmen, D. "Design of optimum response surface experiments for the adsorption of acetic, butyric, and oxalic acids on Amberlyst A21", Journal of Dispersion Science and Technology, 39(2), pp. 305–309, 2018. https://doi.org/10.1080/01932691.2017.1316208

[18] Rizzioli, F., Battista, F., Bolzonella, D., Frison, N. "Volatile Fatty Acid Recovery from Anaerobic Fermentate: Focusing on Adsorption and Desorption Performances", Industrial & Engineering Chemistry Research, 60(37), pp. 13701–13709, 2021. https://doi.org/10.1021/acs.iecr.1c03280

[19] Ozturk, G., Silah, H. "Adsorptive Removal of Remazol Brilliant Blue R from water by using a macroporous polystyrene resin: Isotherm and kinetic studies", Environmental Processes, 7(2), pp. 479–492, 2020. https://doi.org/10.1007/s40710-020-00429-4

[20] Rebecchi, S., Pinelli, D., Bertin, L., Zama, F., Fava, F., Frascari, D. "Volatile fatty acids recovery from the effluent of an acidogenic digestion process fed with grape pomace by adsorption on ion exchange resins", Chemical Engineering Journal, 306, pp. 629–639, 2016. https://doi.org/10.1016/j.cej.2016.07.101

[21] Sigma-Aldrich "Amberlyst® A21 free base, (216410)", [online] Available at: https://www.sigmaaldrich.com/TR/en/product/aldrich/216410 [Accessed: 10 June 2022]

[22] Lagergren, S. "About the Theory of So-Called Adsorption of Soluble Substance", Kungliga Svenska Vetenskapsakademiens Handlingar, 24, pp. 1–39, 1898.

[23] Ho, Y. S., Mckay, G. "Kinetic Models for the Sorption of Dye from Aqueous Solution by Wood", Process Safety and Environmental Protection, 76(2), pp. 183–191, 1998. https://doi.org/10.1205/095758298529326

[24] Ilgen, O., Dulger, H. S. "Removal of Oleic Acid from Sunflower Oil on Zeolite 13X: Kinetics Equilibrium and Thermodynamic Studies", Industrial Crops and Products, 81, pp. 66–71, 2016. https://doi.org/10.1016/j.indcrop.2015.11.050

[25] Jamal, Y., Luo, G., Kuo, C. H., Rabie, A., Boulanger, B. O. "Sorption Kinetics, Thermodynamics and Regeneration for Lipid Feedstock Deacidification Using a Mixed-Bed Ion-Exchange Resin", Journal of Food Process Engineering, 37(1), pp. 27–36, 2014. https://doi.org/10.1111/jfpe.12056

[26] Langmuir, I. "The Adsorption of Gases on Plane Surfaces of Glass Mica and Platinum", Journal of the American Chemical Society, 40(9), pp. 1361–1403, 1918. https://doi.org/10.1021/ja02242a004

[27] Freundlich, H. M. F. "Over the adsorption in solution", Journal of Physical Chemistry, 57, pp. 385–470, 1906.

[28] Dubinin, M. M., Radushkevich, L. V. "Equation of the characteristic curve of activated charcoal", Chemistry Central Journal, 1, pp. 875–889, 1947.

[29] Zhou, X. "Correction to the calculation of Polanyi potential from Dubinnin-Rudushkevich equation", Journal of Hazardous Materials, 384, 121101, 2020. https://doi.org/10.1016/j.jhazmat.2019.121101

[30] Guler, U. A., Sarioglu, M. "Removal of tetracycline from wastewater using pumice stone: equilibrium kinetic and thermodynamic studies", Journal of Environmental Health Science and Engineering, 12(1), 79, 2014. https://doi.org/10.1186/2052-336X-12-79

[31] Cheng, W., Liu, G., Wang, X., Han, L. "Adsorption removal of glycidyl esters from palm oil and oil model solution by using acid-washed oil palm wood-based activated carbon: kinetic and mechanism study", Journal of Agricultural and Food Chemistry, 65(44), pp. 9753–9762, 2017. https://doi.org/10.1021/acs.jafc.7b03121

[32] Mhadmhan, S., Yoosuk, B., Chareonteraboon, B., Janetaisong, P., Pitakjakpipop, P., Henpraserttae, S., Udomsap, P. "Elimination of free fatty acid from palm oil by adsorption process using a strong base anion exchange resin", Separation and Purification Technology, 310, 123211, 2023. https://doi.org/10.1016/j.seppur.2023.123211